


# Device Characteristics of Bulk-Heterojunction Polymer Solar Cells are Independent of Interfacial Segregation of Active Layers

He Wang,<sup>†,‡</sup> Enrique D. Gomez,<sup>†</sup> Jongbok Kim,<sup>†</sup> Zelei Guan,<sup>‡</sup> Chernu Jaye,<sup>§</sup> Daniel A. Fischer,<sup>§</sup> Antoine Kahn,<sup>‡</sup> and Yueh-Lin Loo<sup>\*,†</sup>

<sup>†</sup>Department of Chemical and Biological Engineering and <sup>‡</sup>Department of Electrical Engineering, Princeton University, Princeton, New Jersey 08544, United States

<sup>§</sup>Materials Science and Engineering Laboratory, National Institute of Standards and Technology, Gaithersburg, Maryland 20899, United States

 Supporting Information

**KEYWORDS:** polymer solar cells, interfacial segregation, delamination, vertical phase separation

Thin films of polymer blends comprising two or more chemically incompatible species spontaneously phase segregate, yielding lateral domains whose sizes are dictated by the details of deposition and subsequent processing conditions.<sup>1–4</sup> The constituents of such polymer blends can also preferentially segregate to the film surface and substrate interface, resulting in compositional heterogeneities along the film normal. This phenomenon of interfacial segregation<sup>2,3</sup> is attributed to interfacial free energy differences and is generally observed in thin films comprising blends of random-coil polymers. Interfacial segregation has been, for example, studied extensively and is well-understood for thin films comprising blends of commodity thermoplastics, like polystyrene and poly(methyl methacrylate) or polystyrene and poly(vinyl pyridine).<sup>4</sup> In comparison, interfacial segregation in thin films comprising rodlike, conjugated polymers appears to be more complex given the constituents' tendencies to crystallize.<sup>5–9</sup>

Thin films comprising functional conjugated polymer blends play an important role in organic electronic devices. Thin films of poly(3-hexyl thiophene), P3HT, and high-density polyethylene, HDPE, for example, have been explored as active layers in thin-film transistors.<sup>10</sup> Crystallization-induced interfacial segregation occurs during processing, causing P3HT to be expelled to the film surface and substrate interface. Given the dramatic interfacial segregation that takes place, blends comprising P3HT at concentrations as low as 3 wt % remain electrically active and do not incur any degradation in thin-film transistor performance despite high loadings of electrically insulating HDPE.<sup>10</sup>

Blends of P3HT and phenyl-*C*<sub>61</sub>-butyric acid methyl ester, PCBM, often comprise the thin active layers of bulk-heterojunction polymer solar cells. In such blends, both constituent organic semiconductors are electrically active; in-plane and out-of-plane composition heterogeneities are thus believed to strongly influence solar cell performance.<sup>1–3</sup> In particular, in-plane phase separation has been directly correlated with the extents of exciton dissociation and charge recombination, effectively altering device short-circuit current densities.<sup>11,12</sup> Interfacial segregation in the active layers of bulk-heterojunction solar cells is also perceived to influence device characteristics.<sup>5</sup> The preferential segregation of the polymer donor

to the anode-active layer interface, for example, can block electrons and enhance hole collection; both the open-circuit voltage and the short circuit current density have thus been postulated to increase as a consequence. Conversely, preferential segregation of the polymer donor to the cathode should dramatically increase the series resistance, resulting in reduced device performance.

Although the interfacial segregation characteristics of thin films comprising P3HT and PCBM on substrates having different surface energies have been characterized via spectroscopic ellipsometry,<sup>6</sup> near-edge X-ray absorption fine structure spectroscopy (NEXAFS),<sup>7,8</sup> X-ray photoelectron spectroscopy,<sup>5</sup> and electron tomography,<sup>9</sup> their correlations to device characteristics remain to-date unclear. In a recent publication, Yang and co-workers reported enhancements in device characteristics in inverted solar cells compared to conventional devices; the improvements in performance were attributed to preferential accumulation of the electron acceptor at the buried cathode interface.<sup>5</sup> Given the inverted architecture, however, characteristically different hole and electron transport layers – V<sub>2</sub>O<sub>5</sub> as opposed to the commonly employed poly(3,4-ethylenedioxythiophene):poly(styrene-sulfonate), PEDOT:PSS; and Cs<sub>2</sub>CO<sub>3</sub> as opposed to Ca, respectively – had to be employed to alter the work functions of the electrodes for appropriate charge collection. Since subtle differences in device architectures and energy levels of charge selective layers can influence device characteristics,<sup>13,14</sup> it is unclear whether the differences in interfacial segregation is the sole factor contributing to the disparity in solar cell performance.

Germack and co-workers intentionally induced variations in the composition at the organic active layer-electrode interface by employing hydrogenated and fluorinated PEDOT:PSS hole transport layers in P3HT:PCBM bulk-heterojunction conventional solar cells.<sup>15</sup> Unlike in the prior report, however, the device performance was independent of differences in interfacial segregation. Such discrepancies in the literature point to the difficulties and challenges associated with determining whether and how

**Received:** January 31, 2011

**Revised:** March 17, 2011

**Published:** March 30, 2011

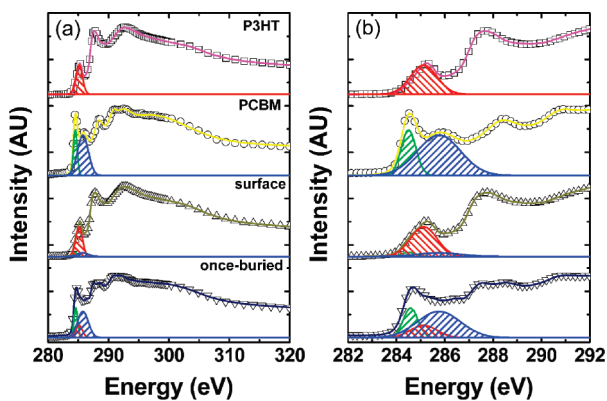


**Figure 1.** (a) Pre- and postedge NEXAFS PEY spectra for films of P3HT, PCBM, and P3HT:PCBM at the surface and the once-buried interface; (b) magnification of the C1s to  $\pi^*$  regions. Open symbols represent experimental data and solid lines represent the sum of the individual fitted peaks. The contributions of P3HT (285.1 eV; red) and PCBM (284.5 eV and 285.8 eV; green and blue) are highlighted. The spectra are displaced along the y-axis for clarity.

interfacial segregation within solar cell active layers influence device performance, and highlight the need for a method to unambiguously elucidate the role of such compositional heterogeneities on solar cell operation.

In this communication, we highlight the use of a simple and straightforward delamination and transfer method to manipulate the bulk-heterojunction active layers of polymer solar cells. Delaminating and flipping the functional organic layers of existing solar cells have allowed us to reverse the interfacial segregation of the active layers; transferring the reversed films onto an otherwise analogous device platform has thus enabled us to unambiguously probe the sole contributions of interfacial segregation on device performance without having to introduce a different device architecture or any new carrier selective layers.

We have chosen to employ the same model system comprising P3HT and PCBM as the electron donor and acceptor, respectively. NEXAFS experiments conducted in partial electron yield (PEY; depth sensitivity several nm)<sup>16–18</sup> mode provides quantification of the mass compositions at the surface and the once-buried interface of P3HT:PCBM thin films.<sup>8</sup> Figure 1a contains PEY NEXAFS spectra collected at the carbon edge and at the “magic” incident angle of 55° of neat films of P3HT and PCBM and those acquired at the exposed surface and the once-buried interface of a thin film comprising P3HT and PCBM. This thin film was processed in the same manner with which P3HT:PCBM bulk-heterojunction active layers are processed. The spectrum of the once-buried interface of the thin film was acquired after it had been delaminated from the glass substrate onto which the blend was initially spin coated. The C1s to  $\pi^*$  transition regions of each spectrum (283 to 287 eV) are magnified for clarity in Figure 1b. Comparison of the NEXAFS spectra of neat P3HT and PCBM indicates differences in the C1s to  $\pi^*$  transitions. Specifically, a single, sharp resonance is observed at 285.1 eV for P3HT whereas two resonances, located at 284.5 and 285.8 eV are identified for PCBM.<sup>8</sup> NEXAFS thus provides unique chemical identifications for P3HT and PCBM. Comparison of the spectra acquired at the exposed surface and the once-buried interface of the P3HT:PCBM thin film with those of the neat constituents allows deconvolution of the  $\pi^*$  resonances attributable to P3HT and PCBM.<sup>8</sup> We determined the C1s to  $\pi^*$  intensities attributable to P3HT to be 92 and 39% at the exposed surface and the once-buried interfaces,

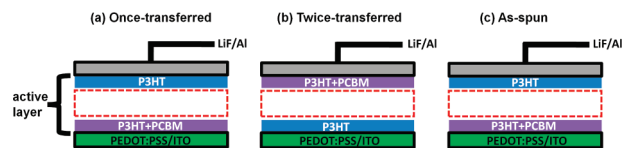


**Figure 2.** Schematic illustration of P3HT:PCBM bulk-heterojunction polymer solar cells having (a) a once-transferred, (b) twice-transferred, and (c) an as-spun P3HT:PCBM active layer.

respectively, corresponding to 97 and 65 wt % P3HT given the molar masses and densities of P3HT and PCBM.<sup>19</sup> We estimated the error in the compositions to be  $\pm 3$  wt % conservatively based on uncertainties associated with spectral deconvolution and data fitting. Consistent with prior reports that P3HT preferentially segregates to the film surface,<sup>5–8</sup> the exposed surface comprises largely of P3HT. The once-buried interface is only slightly enhanced in P3HT compared to the composition of the cosolution from which the film was cast (55 wt %).

To assess the influence of interfacial segregation in the active layers on device performance, we incorporated the NEXAFS-characterized thin film into functional solar cells. The ability to peel and transfer thin layers<sup>20,21</sup> comprising blends of P3HT and PCBM greatly modularizes device fabrication and allows us to uniquely probe the influence of interfacial segregation on solar cell characteristics. Figure 2 illustrates the device geometries employed in our study. All devices were constructed using the conventional architecture in which the bottom indium tin oxide (ITO) electrodes serve as anodes and the top aluminum electrodes serve as cathodes. Thin PEDOT:PSS layers (ca. 20 nm) were deposited on ITO to promote hole transport to the anodes. In devices comprising the once-transferred P3HT:PCBM thin films, the active layers retain its original interfacial segregation characteristics that is shown in Figure 1. Devices with twice-transferred P3HT:PCBM active layers were constructed by first delaminating the as-spun P3HT:PCBM films and turning them over before transferring them onto PEDOT:PSS. This manipulation resulted in the reversed composition profile; the surface that was once exposed on the as-spun film is now buried and is in direct contact with PEDOT:PSS. To ensure reliable electrical contact between the polymer films and the underlying PEDOT:PSS, we imposed a 3 min thermal anneal at 100 °C during the transfer of polymer films. For reference, we also spin-coated the same cosolution of P3HT and PCBM directly onto PEDOT:PSS coated ITO; the as-spun active layer thus possesses the same composition profile as the once-transferred active layer. The as-spun active layer of P3HT and PCBM was also subjected to thermal annealing at 100 °C for 3 min prior to top electrode deposition for consistency. Although we recognize that annealing at 100 °C for 3 min is suboptimal for achieving the maximum efficiency in our devices, this annealing condition was employed to suppress changes in the vertical phase separation of the active layers with thermal annealing during transfer. LiF (ca. 1 nm) and Al (60 nm) were deposited on the active layers as the cathode. Aside from the delamination and transfer of P3HT:PCBM films, device fabrication and testing were all carried out in the glovebox to prevent oxidation of LiF/Al cathodes.

To ascertain the impact of this short anneal, we conducted X-ray photoelectron spectroscopy (XPS; depth sensitivity ca. 5–10 nm for polymers) on the surface of the once- and twice-transferred P3HT:PCBM thin films before and after thermal annealing. This short anneal does not affect the composition at the surface of the once-transferred film, presumably because this surface already comprises crystalline and preferentially oriented P3HT (see the Supporting

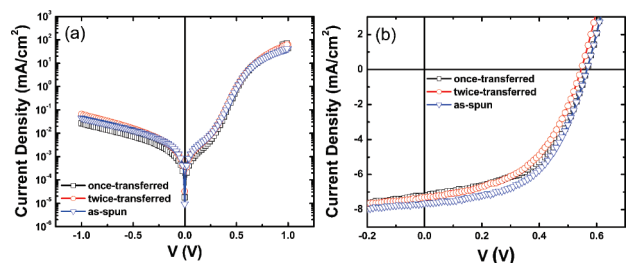


**Figure 3.**  $J$ – $V$  characteristics acquired (a) in the dark and (b) under illumination of representative polymer solar cells with once-transferred (squares), twice-transferred (circles), and as-spun (triangles) P3HT:PCBM bulk-heterojunction active layers.

**Table 1.** Photovoltaic Characteristics of Polymer Solar Cells Tested

|                   | $V_{oc}$ (V)    | $J_{sc}$ (mA/cm <sup>2</sup> ) | efficiency (%)  | fill factor     |
|-------------------|-----------------|--------------------------------|-----------------|-----------------|
| once-transferred  | $0.57 \pm 0.01$ | $7.41 \pm 0.45$                | $2.21 \pm 0.20$ | $0.52 \pm 0.02$ |
| twice-transferred | $0.55 \pm 0.01$ | $7.38 \pm 0.04$                | $1.93 \pm 0.05$ | $0.48 \pm 0.01$ |
| as-spun           | $0.57 \pm 0.01$ | $7.26 \pm 0.54$                | $2.26 \pm 0.14$ | $0.55 \pm 0.02$ |

Information). This short anneal, however, does increase the surface PCBM composition of the twice-transferred film by 10 wt %, likely because PCBM diffusion in the amorphous regions of P3HT at 100 °C is not negligible.<sup>22</sup> Despite this modest change in the surface composition of the twice-transferred film, the direction of asymmetry in the interfacial compositions is preserved and, if anything, its magnitude further accentuated, so this short anneal should not affect the conclusions drawn herein.

Figure 3 contains the dark and illuminated characteristics of representative conventional bulk-heterojunction solar cells having as-spun, once-transferred and twice-transferred active layers. Four to twelve devices were tested in each case; the spread in the device characteristics were averaged to produce the mean and standard deviation values reported in Table 1. The  $J$ – $V$  characteristics acquired in the dark for all devices exhibit excellent rectification with rectification ratios greater than  $1 \times 10^3$ . Under illumination, the devices exhibit comparable average open-circuit voltage ( $V_{oc}$ ) of  $0.56 \pm 0.01$  V. This value is consistent with typical  $V_{oc}$ 's reported for P3HT:PCBM bulk-heterojunction devices, and has been reported to depend on the work function difference of the electrodes and the energy level difference between the highest occupied molecular orbital of P3HT and lowest unoccupied molecular orbital of PCBM.<sup>3</sup> The short-circuit current densities ( $J_{sc}$ ) of the devices are also comparable at  $7.35 \pm 0.44$  mA/cm<sup>2</sup>, resulting in comparable efficiencies across all the devices ( $2.16 \pm 0.21\%$ ).

Given that P3HT is partial to hole transport, we had initially expected preferential segregation of P3HT to the cathode interface in devices with as-spun and once-transferred active layers to exhibit high series resistance, ultimately manifesting in reduced short-circuit current densities. It follows that devices with twice-transferred active layers should exhibit improved current densities and working voltages compared to devices with as-spun and once-transferred active layers.<sup>5</sup> That both the dark and illuminated characteristics of our devices are comparable is surprising and indicates that—contrary to common belief—differences in interfacial segregation do not influence device performance.

Although P3HT is greatly enhanced at the cathodes of devices with as-spun and once-transferred active layers, these interfaces

still comprise 3 wt % PCBM. We speculate that this fractional amount of PCBM at the active layer-cathode interface can still provide sufficient percolative, low-resistance pathways that enable electron extraction. Our results thus implicate that device characteristics of bulk-heterojunction solar cells are insensitive to the details of interfacial segregation, so long as the active layer-electrode interface does not comprise a continuous layer of the organic semiconductor constituent that hinders charge extraction. As negative control experiments, we fabricated and tested bulk-heterojunction solar cells in which a thin but continuous layer of PCBM (ca. 12–14 nm) was first spin coated on the anode and the active layer was subsequently transferred onto the PCBM layer. The characteristics of these devices are summarized in the Supporting Information. As expected, the performance of such devices is severely limited by high series resistance, presumably because holes are entirely blocked from reaching the anode. Interestingly, transferring a thin but continuous P3HT layer (ca. 8–9 nm) onto the active layer before cathode deposition does not significantly influence device characteristics. This observation implies an asymmetry in charge transport; our experiments suggest that P3HT is less effective at blocking electron transport to the cathode compared to PCBM at blocking hole transport to the anode.

## ■ ASSOCIATED CONTENT

**S Supporting Information.** Detailed procedures for NEXAFS analysis, delamination and transfer of active layers, construction and testing of solar cells; XPS and NEXAFS fluorescence yield analyses. This material is available free of charge via the Internet at <http://pubs.acs.org/>.

## ■ AUTHOR INFORMATION

### Corresponding Author

\*E-mail: [lloo@princeton.edu](mailto:lloo@princeton.edu).

## ■ ACKNOWLEDGMENT

Funding from ONR (N00014-08-1-1175) supported this work. We also acknowledge partial funding from the SOLAR Initiative (DMR-1035217) and MRSEC program (DMR-0819860) at the NSF. A.K. also acknowledges support from DOE (DEFG02-04ER46165 and DE-S0001084).

## ■ REFERENCES

- (1) Kippelen, B.; Bredas, J.-L. *Energy Environ. Sci.* **2009**, *2*, 251.
- (2) Lee, S. S.; Loo, Y.-L. *Annu. Rev. Chem. Biomol. Eng.* **2010**, *1*, 59.
- (3) Gomez, E. D.; Loo, Y.-L. *J. Mater. Chem.* **2010**, *20*, 6604.
- (4) Geoghegan, M.; Krausch, G. *Prog. Polym. Sci.* **2003**, *28*, 261.
- (5) Xu, Z.; Chen, L.-M.; Yang, G.; Huang, C.-H.; Hou, J.; Wu, Y.; Li, G.; Hsu, C.-S.; Yang, Y. *Adv. Funct. Mater.* **2009**, *19*, 1227.
- (6) Campoy-Quiles, M.; Ferenczi, T.; Agostinelli, T.; Etchegoin, P. G.; Kim, Y.; Anthopoulos, T. D.; Stavrinou, P. N.; Bradley, D. D. C.; Nelson, J. *Nat. Mater.* **2008**, *7*, 158.
- (7) Germack, D. S.; Chan, C. K.; Hamadani, B. H.; Richter, L. J.; Fischer, D. A.; Gundlach, D. J.; DeLongchamp, D. M. *Appl. Phys. Lett.* **2009**, *94*, 233303.
- (8) Guan, Z.-L.; Kim, J. B.; Wang, H.; Jaye, C.; Fischer, D. A.; Loo, Y.-L.; Kahn, A. *Org. Electron.* **2010**, *11*, 1779.
- (9) van Bavel, S. S.; Sourty, E.; de With, G.; Loos, J. *Nano Lett.* **2009**, *9*, 507.

- (10) Goffri, S.; Muller, C.; Stingelin-Stutzmann, N.; Breiby, D. W.; Radano, C. P.; Andreasen, J. W.; Thompson, R.; Janssen, R. A. J.; Nielsen, M. M.; Smith, P.; Sirringhaus, H. *Nat. Mater.* **2006**, *5*, 950.
- (11) Kim, C. S.; Tinker, L. L.; DiSalle, B. F.; Gomez, E. D.; Lee, S.; Bernhard, S.; Loo, Y.-L. *Adv. Mater.* **2009**, *21*, 3110.
- (12) Kim, J. B.; Allen, K.; Oh, S. J.; Lee, S.; Toney, M. F.; Kim, Y. S.; Kagan, C. R.; Nuckolls, C.; Loo, Y.-L. *Chem. Mater.* **2010**, *22*, 5762.
- (13) Hau, S. K.; Yip, H.-L.; Acton, O.; Baek, N. S.; Ma, H.; Jen, A. K. Y. *J. Mater. Chem.* **2008**, *18*, 5113.
- (14) Yip, H.-L.; Hau, S. K.; Baek, N. S.; Ma, H.; Jen, A. K. Y. *Adv. Mater.* **2008**, *20*, 2376.
- (15) Germack, D. S.; Chan, C. K.; Kline, R. J.; Fischer, D. A.; Gundlach, D. J.; Toney, M. F.; Richter, L. J.; DeLongchamp, D. M. *Macromolecules* **2010**, *43*, 3828.
- (16) Stohr, J. *NEXAFS Spectroscopy*; Springer: Berlin, 1992.
- (17) Krapchetov, D. A.; Ma, H.; Jen, A. K. Y.; Fischer, D. A.; Loo, Y.-L. *Langmuir* **2005**, *21*, 5887.
- (18) Krapchetov, D. A.; Ma, H.; Jen, A. K. Y.; Fischer, D. A.; Loo, Y.-L. *Langmuir* **2008**, *24*, 851.
- (19) The mass densities for P3HT and PCBM are 1.1 and 1.5 g/cm<sup>3</sup>, respectively; from ref 9.
- (20) Kim, J. B.; Lee, S.; Toney, M. F.; Chen, Z.; Facchetti, A.; Kim, Y. S.; Loo, Y.-L. *Chem. Mater.* **2010**, *22*, 4931.
- (21) Loo, Y.-L.; Someya, T.; Baldwin, K. W.; Bao, Z.; Ho, P.; Dodabalapur, A.; Katz, H. E.; Rogers, J. A. *Proc. Natl. Acad. Sci.* **2002**, *99*, 10252.
- (22) Treat, N. D.; Brady, M. A.; Smith, G.; Toney, M. F.; Kramer, E. J.; Hawker, C. J.; Chabynyc, M. L. *Adv. Energy Mater.* **2011**, *1*, 82.